

Title: Normative brain mapping of interictal intracranial EEG to localise epileptogenic tissue

Authors: Peter N Taylor^{1,2,*}, Christoforos A Papasavvas¹, Thomas W Owen¹, Gabrielle M Schroeder¹, Frances E Hutchings¹, Fahmida A Chowdhury², Beate Diehl², John S Duncan², Andrew W McEvoy², Anna Miserocchi², Jane de Tisi², Sjoerd B Vos², Matthew C Walker², Yujiang Wang^{1,2,*}

1. CNNP Lab (www.cnnp-lab.com), Interdisciplinary Computing and Complex BioSystems Group, School of Computing, Newcastle Helix, Newcastle University, UK

2. UCL Queen Square Institute of Neurology & National Hospital for Neurology and Neurosurgery (NHNN), Queen Square, London WC1N 3BG, UK

* denotes equal contribution. yujiang.wang@newcastle.ac.uk peter.taylor@newcastle.ac.uk

Normative brain mapping of interictal intracranial EEG to localise epileptogenic tissue

Peter N. Taylor, Christoforos A. Papasavvas, Thomas W. Owen, Gabrielle M. Schroeder, Frances E. Hutchings, Fahmida A. Chowdhury, Beate Diehl, John S. Duncan, Andrew W. McEvoy, Anna Miserocchi, Jane de Tisi, Sjoerd B. Vos, Matthew C. Walker, Yujiang Wang

Abstract

The identification of abnormal electrographic activity is important in a wide range of neurological disorders, including epilepsy for localising epileptogenic tissue. However, this identification may be challenging during non-seizure (interictal) periods, especially if abnormalities are subtle compared to the repertoire of possible healthy brain dynamics. Here, we investigate if such interictal abnormalities become more salient by quantitatively accounting for the range of healthy brain dynamics in a location-specific manner.

To this end, we constructed a normative map of brain dynamics, in terms of relative band power, from interictal intracranial recordings from 234 subjects (21,598 electrode contacts). We then compared interictal recordings from 62 patients with epilepsy to the normative map to identify abnormal regions. We hypothesised that if the most abnormal regions were spared by surgery, then patients would be more likely to experience continued seizures post-operatively.

We first confirmed that the spatial variations of band power in the normative map across brain regions were consistent with healthy variations reported in the literature. Second, when accounting for the normative variations, regions which were spared by surgery were more abnormal than those resected only in patients with persistent post-operative seizures ($t=-3.6$, $p=0.0003$), confirming our hypothesis. Third, we found that this effect discriminated patient outcomes ($AUC=0.75$ $p=0.0003$).

Normative mapping is a well-established practice in neuroscientific research. Our study suggests that this approach is feasible to detect interictal abnormalities in intracranial EEG, and of potential clinical value to identify pathological tissue in epilepsy. Finally, we make our normative intracranial map publicly available to facilitate future investigations in epilepsy and beyond.

Introduction

Abnormal electrographic activity is a hallmark of many neurological disorders. In focal epilepsy, ictal (seizure) periods commonly display clear pathological dynamics, which is clinically used to localize epileptogenic tissue. However, studies have suggested that interictal dynamics may also hold useful complementary information to identify epileptogenic tissue. For example, interictal spikes, sharp waves, and high frequency oscillations have all been suggested as putative markers (Jacobs et al. 2009, 2010; Stephen V. Gliske et al. 2018b; Klooster et al. 2017; Hufnagel et al. 1994; Rosenow and Lüders 2001; Erin C. Conrad et al. 2020b; Roehri et al. 2018).

Grossly abnormal interictal events, such as interictal spikes, can often be identified visually or algorithmically. However, existing techniques may struggle to distinguish more subtle aberrations from the vast repertoire of possible healthy brain dynamics. Example healthy brain dynamics include beta oscillations, commonly seen in motor areas (Morillon et al. 2019; Hillebrand et al. 2012), and gamma activity in occipital and temporal areas (Niso et al. 2016; Keitel and Gross 2016). Other spatial profiles include alpha oscillations in occipital and parietal areas (Niso et al. 2016; Frauscher et al. 2018), delta in the temporal lobe (Keitel and Gross 2016; Frauscher et al. 2018; Niso et al. 2019), and theta in superior frontal areas (Groppe et al. 2013; Ishii et al. 1999). In this work, we suggest that neural activity in these frequencies may also represent pathological activity if it occurs in brain regions that do not normally feature these frequencies. Conversely, a lack of power in typical frequencies of a particular brain region may also indicate pathological activity. Thus, identifying such subtle pathological activities requires the consideration of the spatial distribution of 'normal' electrographic activity.

One approach to account for normal spatial variations is to construct a normative map, which describes the healthy spatial profile and ranges of the feature of interest (in this case the band power of different frequency bands). Such an approach is common and well-accepted in neuroimaging of brain structural abnormalities: patients are often normalised against healthy controls to highlight abnormal brain morphology (Whelan et al. 2018) or connectivity (Sinha et al. 2021; Hatton et al. 2020). However, for invasive recordings using intracranial EEG, data from healthy controls are not available. Instead, recent studies suggested using intracranial EEG recorded from areas outside of the putative seizure-generating tissue in patients with epilepsy (Frauscher et al. 2018; Betzel et al. 2019). Specifically, (Frauscher et al. 2018) conclude that this approach yields a normative map of brain dynamics that is consistent with data from animal models and other recording modalities.

In this study, we therefore follow this proposed approach to generate a normative map of band power across the brain using intracranial recordings from 234 subjects with 21,598 recording contacts from outside the seizure onset and initial propagation zone. We first quantify the spatial distributions of normative band power and confirm agreement with previous data. Then, using a separate cohort of 62 patients with epilepsy, we show that accounting for the normative map allows us to identify epileptogenic tissue and subsequently predict patient surgical outcomes.

Methods

Patients

Two main cohorts were studied here. The RAM normative cohort consisted of 234 subjects with epilepsy undergoing presurgical evaluation with intracranial EEG to localise seizure onset. As part of the intracranial EEG monitoring, the subjects were also participating in an experimental study on memory (data collected up to year 3; <http://memory.psych.upenn.edu/RAM>). As stated in the project's website "Informed consent has been obtained from each subject to share their data, and personally identifiable information has been removed to protect subject confidentiality". The original research protocol for data acquisition was approved by the relevant bodies at the participating institutions. Furthermore, the University Ethics Committee at Newcastle University approved the analysis of this dataset (Ref: 12721/2018). The normative recordings were obtained in the preparatory phase, several minutes before a memory task.

The UCLH epilepsy cohort consisted of 62 patients with epilepsy undergoing presurgical evaluation with invasive intracranial EEG to localise seizure onset. All patients also had pre-surgical, pre-implantation T1-weighted (T1w) MRI. All patients had either CT or T1w MRI whilst implanted electrodes were in place. The majority of patients had post operative T1w MRI (N=61). For the single patient without post-operative MRI, the detailed surgery report described the brain areas resected. At follow-up of 12 months, 33 patients were free of disabling seizures and 29 had persistent seizures. Follow-up outcomes were defined as described previously according to the ILAE classification (Durnford et al. 2011). A subset of this cohort has been studied previously (Wang et al. 2020). All data were anonymised and exported, then analysed under the approval of the Newcastle University Ethics Committee (2225/2017). Detailed patient metadata are shown in Supplementary Information S1 and summarised in table 1. No substantial or significant differences were present between outcome groups in age, sex, lobe of resection, side of resection, or number of electrode contacts.

Table 1: Summary of patient data.

	ILAE1,2	ILAE3+	Test statistics
N (%)	33 (53%)	29 (47%)	
Age (mean,SD)	32.3 (10.7)	33.0 (8.8)	$p=0.8017$, $t=-0.2522$
Sex (M,F)	15,18	17,12	$p=0.8759$, $\chi^2=0.0244$
Temporal, extratemporal	21,12	15,14	$p=0.5987$, $\chi^2=0.277$
Side (Left, Right)	18,15	16,13	$p=0.17$, $\chi^2=1.8829$
Number of electrode contacts (mean, SD)	71.1 (24.3)	65.9 (23.3)	$p=0.3984$, $t=0.8505$

MRI processing for electrode localisation and resection delineation

Electrode contacts for all subjects were localised to regions of interest defined according to a parcellation. To ensure robustness of our findings we investigated four separate parcellations at

different resolutions, where higher resolutions are subdivisions of lower resolutions. These parcellations have been described previously (Hagmann et al. 2008) and have been used for normative intracranial analysis (Betzel et al. 2019). Due to different levels of available data, our technique for localisation of electrode contacts to regions differed slightly between the RAM and UCLH datasets. In the RAM data, electrode contact locations are publicly available as Talairach space coordinates, which we converted to MNI space (Lancaster et al. 2007). We next reconstructed an MNI space brain using FreeSurfer, matched each of the four parcellations to that surface using `mri_surf2surf`, obtained the labels and matched each contact to the closest volumetric region of interest (minimum euclidean distance using custom code in matlab). For UCLH data we performed broadly the same procedure but performed the processing in native space. Performing native space processing was possible as the pre-operative T1w MRI was available along with the CT/MRI scan to mark electrode contacts as described previously (Wang et al. 2020; Hamilton et al. 2017). To identify which regions were removed/spared by surgery we linearly registered the post-operative T1w scan to the pre-operative scan and manually delineated the resected tissue as a mask described previously (Wang et al. 2020; Taylor et al. 2018). Electrode contacts were defined as removed if they were within 5mm of the mask as in our prior work (Wang et al. 2020). In each patient, regions were defined as removed if >25% of contacts within the region were removed. Regions were considered spared if and only if no contacts within that region were removed. In cases where a region contained > 0% and \leq 25% of removed contacts, it was considered uncertain and the region was not included in analysis.

Intracranial EEG data and processing

To create a normative baseline of intracranial EEG (iEEG) spectral properties we used the RAM dataset, and extracted 70 seconds of iEEG recording from relaxed wakefulness (shortly before a memory task) for each subject. We excluded channels that were labelled as seizure onset zone, early propagation zone, brain lesions, or bad contacts. The extracted EEG signals from the remaining channels were visually inspected for recording artefacts, and recording channels located in white matter were also excluded, resulting in a final set of 21,598 channels across 234 subjects.

We further used a separate iEEG dataset from UCLH to compare and score against the normative baseline. Again, we retrospectively extracted 70 seconds of interictal iEEG recording for each subject, at least 2h away from seizures. Where possible, the recording was obtained at around 2pm in the afternoon to maximise the likelihood of wakefulness. Due to the retrospective design, it was not possible to determine the exact brain state. To demonstrate robustness, we also present results for two further time segments at least 2h away from seizures and 4h away from other time segments at around 9am and 7pm where possible. For the UCLH dataset, we included all grey matter channels (i.e. even those in seizure onset zone, propagation zone, and irritative zones). We only excluded artefactual channels and recording channels in white matter, resulting in 4256 channels across 62 patients.

After applying a common average reference to all recordings in all subjects, we estimated the power spectral density with Welch's method (2 s window, 1 s overlap) in each 70 s recording. The average band power within five frequency bands of interest were then calculated using the

'bandpower' function in matlab. The following ranges were defined, delta (δ 1-4 Hz), theta (θ 4-8 Hz), alpha (α 8-13 Hz), beta (β 13-30 Hz) and gamma (γ 30-80 Hz). In the gamma band, data between 47.5 Hz to 52.5 Hz and 57.5 Hz to 62.5 Hz was excluded to avoid power line artifacts in both the US and UK recordings. Band power estimates were then \log_{10} transformed and normalised to sum to 1 for each contact (i.e. L1 norm). These transformed and normalised values represent the relative band power used throughout results. Each subject therefore has a value of relative band power assigned to each contact and each frequency band.

Normative map generation

To obtain a normative distribution of relative band power in a particular frequency band and brain region, we first assigned each electrode contact from each subject in the RAM dataset to a grey matter region, as described above. One contact can only be assigned to a single (nearest) region. If multiple contacts from the same subject were assigned to the same region, then we averaged the relative band powers to obtain single values of relative band power per region and frequency band per patient. If zero contacts were assigned to a region in a particular subject, then the region was considered to have no coverage and the relative band powers were set to NaN (not a number) for that subject and region. The normative distribution of relative band power in a region (in a particular frequency band) was then obtained as the distribution of relative band powers of all RAM subjects with coverage in that region.

To visualise the normative map, we plot the mean of the distribution of relative band powers in a particular region and frequency band across normative subjects (see Fig. 1).

Scoring patients to the normative map

To score the UCLH patient cohort against the normative map, we followed a similar approach in mapping the electrodes to brain regions. Electrode contacts for a given patient were localised to a single brain region (i). Where multiple contacts localised to the same region the mean band power value across contacts was used. This allows estimation of the band power in a given region (i), in a given frequency band (j), for a given patient.

To estimate the abnormality of a region's relative band power in the UCLH dataset from the normative map we computed the absolute z-score:

$$|z_{i,j}| = \left| \frac{x_{i,j} - \mu_{i,j}}{\sigma_{i,j}} \right|$$

where i represents the region, and j the frequency band of interest, x is the band power value for an individual patient, μ and σ are the mean and standard deviations band powers of the normative map.

Statistical analysis

In comparing the values between resected and spared regions for any patient in the UCLH dataset and frequency band, we used the distinguishability statistic (D_{RS}), which is the area under the receiver operating curve, and equivalent to the normalised Mann-Whitney U statistic (see Wang

et al. 2020; Ramaraju et al. 2020; Bernabei et al. 2020). A D_{RS} value greater than 0.5 indicates that spared regions were more abnormal (higher absolute z-score) than resected regions, whereas D_{RS} values below 0.5 indicates the opposite - i.e. resected regions were more abnormal.

Hypothesising that resected regions would be more abnormal than spared regions in good outcome patients, we tested for $D_{RS} < 0.5$ in good outcome patients using a left tailed one sample t-test. In contrast, we hypothesised the opposite effect in poor outcome patients and tested $D_{RS} > 0.5$ using a one sample right tailed t-test. Finally, we hypothesised greater D_{RS} values in poor outcome patients than good outcome patients, and tested with a two sample left tailed t-test.

Statistical significance is reported for $p < 0.05$ for reference. Effect sizes are reported throughout as t-statistics or as area under the receiver operating characteristic curve (AUC).

Data and code availability

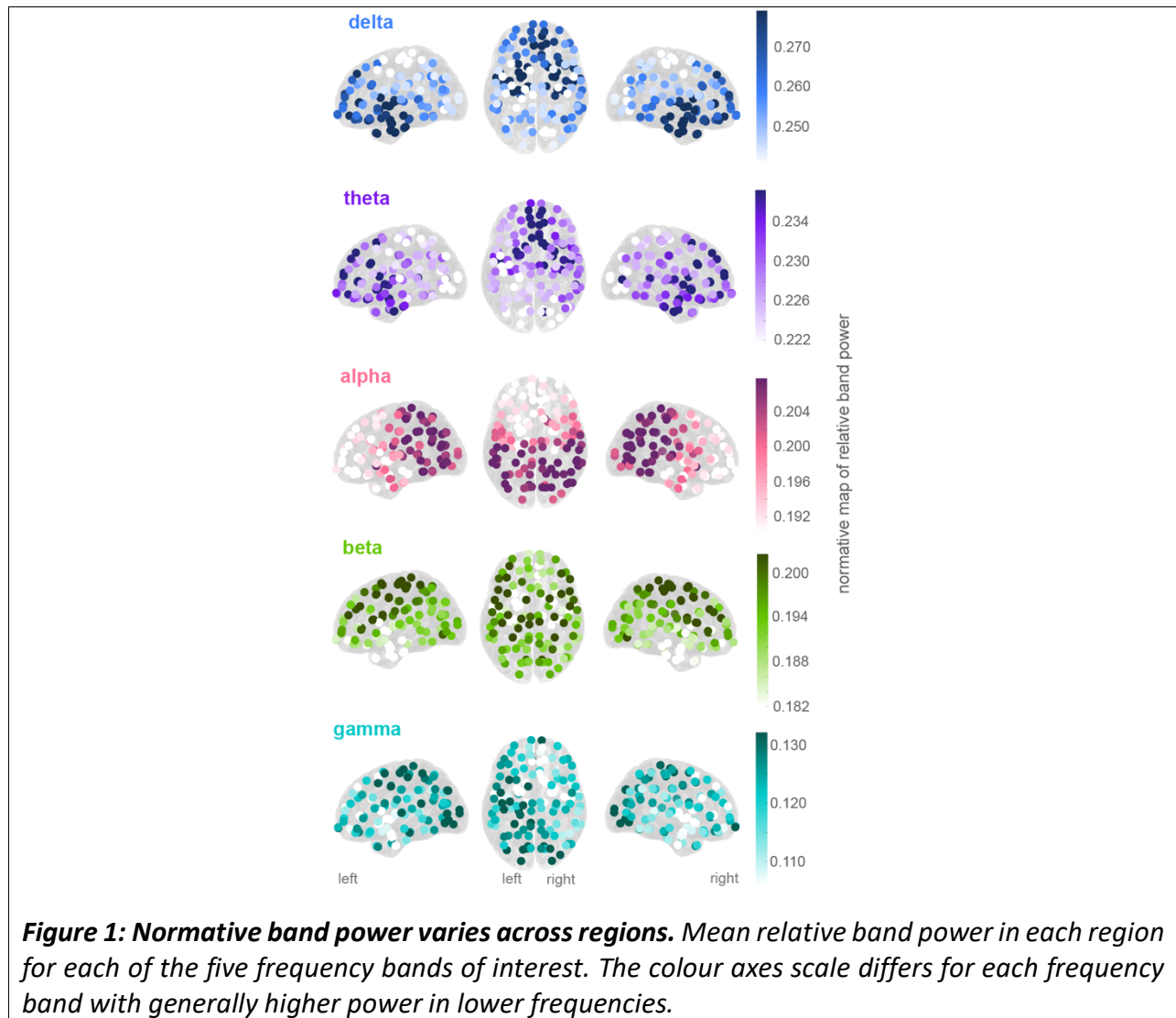
Preprocessed data and analysis code will be made available upon acceptance of the manuscript.

Results

Normative maps show spatial organisation of band power

We constructed normative maps of relative power in five frequency bands (δ : 1-4Hz, θ : 4-8Hz, α : 8-13Hz, β : 13-30Hz, and γ : 30-80Hz). To construct the normative maps, we used 70 seconds of interictal intracranial EEG recordings from 21,598 electrode contacts outside of the seizure onset and initial propagation zone across 234 subjects. The 70 second segments were recorded while the subjects were awake and preparing for a cognitive task experiment. We derived the relative band power for five main frequency bands in all contacts. Each contact was then assigned to one of 128 regions of interest (ROIs) from the Lausanne scale60 atlas (Hagmann et al. 2008), yielding a normative distribution of relative band power in each ROI.

The resulting normative maps of the mean relative band power for each frequency band are shown in Figure 1A. Several distinct patterns can be observed; for example, relative delta power is most prominent in the anterior temporal and anterior frontal regions, while relative alpha power is prominent in parietal and occipital regions. Note that lower frequencies generally have higher relative power (the colour axes scale differs for each frequency band in Fig. 1A). Finally, the overall gradient of the normative maps also display a striking symmetry between the left and right hemispheres.



Normative maps highlight abnormalities in individual patients

We then turned our attention to a cohort of patients from UCLH with refractory focal epilepsy who underwent presurgical evaluation with intracranial EEG. We used the normative maps as a baseline to identify aberrations in each ROI for individual patients.

We use an example patient to illustrate the process. Patient ID 1216 had electrode contacts placed in the temporal, parietal and occipital lobes. Those electrodes were localised to corresponding ROIs (black circles in Figure 2A). We also show the interictal EEG time series of two example contacts in two different regions in Fig. 2A. The first region is the left middle temporal gyrus 2 (LMTG2), which is far away from the seizure onset zone in this patient. The second region is the left lateral occipital gyrus 2 (LLOG2), which is the seizure onset zone as determined by the presurgical evaluation.

On visual inspection, the two time series are not qualitatively different. However, following extraction of relative band power from the 70 s interictal recording for each of the two regions,

and subsequent standardisation to the normative distributions in each frequency band (violin plots in Fig. 2B), the LLOG2 region showed substantial deviations, particularly in the theta band (absolute z-score of 2.99). In contrast, the LMTG2 region did not display strong deviations in any frequency band ($\lesssim 1$ standard deviation away from the normative distributions).

We repeated the procedure of z-scoring all frequency bands in all ROIs relative to the corresponding normative distributions for example patient 1216. It is conceivable that different frequency bands are abnormal in different regions and subjects. Therefore, to summarise these z-scores across frequency bands, we used the maximum absolute z-score as a measure of the regional level of aberration (Fig. 2C). Taking the maximum essentially summarised the level of interictal band power abnormality whilst allowing for region and subject-specific differences in terms of the frequency band. In this example patient, it is visually clear from Fig. 2C that the level of abnormality is highest in the LLOG2 region, but other occipital regions also presented with a high level of abnormality.

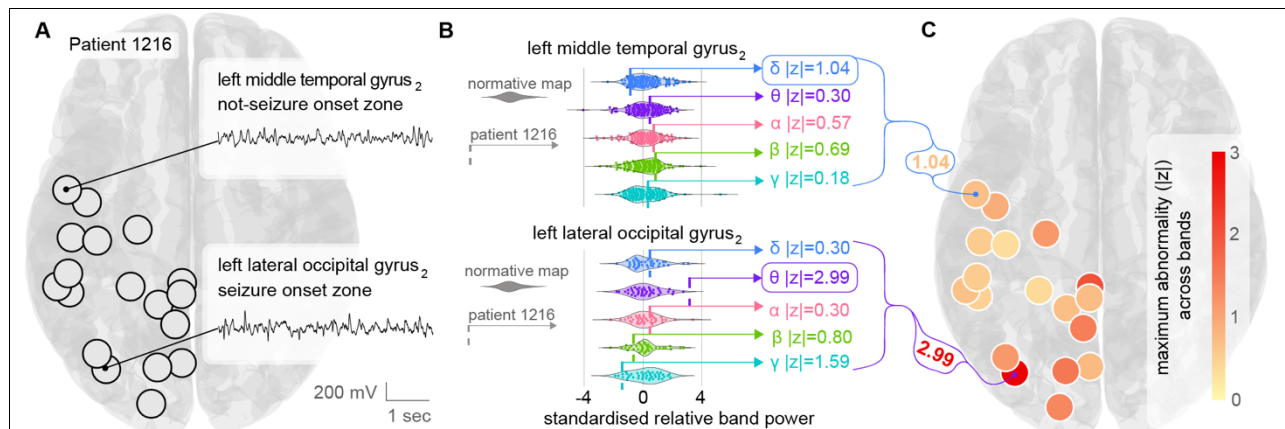


Figure 2: Normative band power as a reference to detect abnormalities in individual patients.

A. Visualisation of the regions covered by the implanted electrodes in an example patient with epilepsy. 18 (black circles) of the 128 regions were sampled by the electrode contacts in this patient. Time series from two example regions are shown that are without obvious epileptiform activity (inset). One example region (left lateral occipital gyrus 2) was the seizure onset zone in this patient. **B.** Relative band power for each of the two regions, across each frequency band is plotted for the normative data (coloured violin plot; each point is a normative subject). Data is standardised (mean subtracted and divided by standard deviation). Relative band power z-score for the patient 1216 is plotted as a vertical dashed line on the same scale. The z-scores indicates that the left middle temporal gyrus is normal in all frequency bands (maximum absolute z-score = 1.04). The left lateral occipital gyrus is more abnormal in theta (maximum absolute z-score = 2.99) and gamma (absolute z-score = 1.59). **C.** Maximum absolute z-score for each region plotted for the patient. Larger values indicate greater abnormality in any frequency band.

Interictal band power abnormality distinguishes epileptogenic tissue

We next postulated that our measure of interictal band power abnormality of a region may serve as a marker of the region's epileptogenicity. We thus hypothesised that the surgical removal of regions with the greatest abnormalities would be associated with post-operative seizure freedom. In contrast, if abnormal regions remain after surgery, we expect to see persistent seizures after surgery. To address this hypothesis, we retrospectively identified which regions were resected by surgery and compared the level of abnormality between surgically resected and spared regions.

The example patient 1216 in Figure 3A,B is the same patient shown in Figure 2. The LLOG2 region was resected, along with other occipital regions. It is visually apparent that the resected regions (circled in black in figure 3B) appear substantially more abnormal than regions which were spared by surgery in this first example patient. The lower panel of Fig. 3B quantifies the difference between the resected and spared regions using the D_{RS} metric that quantifies the Distinguishability of the Resected and Spared regions (Wang et al. 2020; Ramaraju et al. 2020; Bernabei et al. 2020). D_{RS} values close to 0 indicate that resected regions are more abnormal than spared regions. In contrast, if D_{RS} is close to 1, then spared regions are more abnormal than resected regions. A $D_{RS} = 0.5$ indicates that the resected and spared regions are indistinguishable in terms of the level of interictal band power abnormality. Example patient 1216 has a $D_{RS} = 0.14$ (Fig. 3B), indicating that regions removed by surgery were typically more abnormal than regions spared by surgery. This patient was subsequently seizure free upon follow-up.

Interictal band power abnormalities of a second example patient (ID: 910), derived using the same processing and normative analysis, are presented in Figure 3C,D. This patient had an anterior frontal lobe resection. Their resection involved the removal of areas with normal interictal band powers ($|z| \lesssim 1$), whilst highly abnormal regions remained in more posterior parts of the frontal lobe. Analysis using D_{RS} confirms this finding with $D_{RS} = 0.98$, indicating that almost all spared regions were more abnormal than those resected. This example patient continued to have persistent post-operative seizures.

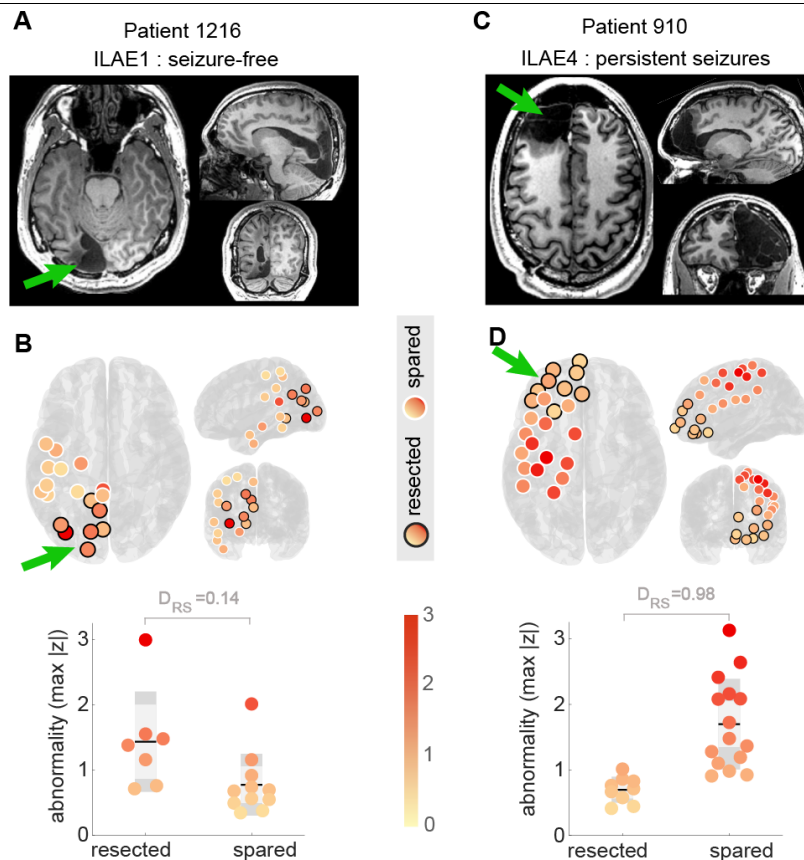


Figure 3: Interictal band power abnormality as a marker of epileptogenic tissue in two example patients. *A, C* Post-operative T1-weighted MRI scans showing the location of the resection as indicated by the green arrow. *B*. Replication of the patient in figure 2 with the regions that were later surgically resected circled in black. Non-resected regions are circled in white. A direct comparison and quantification in the lower panel shows resected regions to be more abnormal than spared. Each data point is a separate region. This patient was seizure free after surgery (ILAE1). *D*. Visualisation of data from a second patient with a frontal lobe implantation. Multiple abnormal regions were present outside the resection and spared by surgery. This patient had had continued post-operative seizures (ILAE4). In both patients the D_{RS} metric quantified the difference between resected and spared regions in terms of their abnormality.

The two patients presented in Figure 3 suggest that the interictal band power abnormality measure may serve as a marker of epileptogenicity, and its ability to distinguish resected from spared tissue (D_{RS}) may subsequently be used to predict seizure-freedom after surgery. In Figure 4A,B we generalise those findings across a cohort of 62 patients. At a group level, patients with persistent seizures (ILAE3+) had substantially and significantly greater D_{RS} values than those who were free of disabling seizures (ILAE1,2) (right tailed t-test $p=0.0003$, $t=-3.6$, $AUC=0.75$, see Fig. 4A,B). Furthermore, D_{RS} values of patients with persistent seizures were substantially and significantly greater than 0.5, suggesting that abnormal regions were spared by surgery in ILAE3+ patients ($p=0.0003$, $t=3.8$, right tail t-test). Values of D_{RS} for ILAE1,2 patients were not

significantly less than 0.5 ($p=0.129$, $t=-1.15$, left tail t-test). Taken together, these group level findings suggest that regions with interictal abnormalities remain after surgery in patients with persistent post-operative seizures. Furthermore, the distinguishability between the resected and spared abnormality (i.e. D_{RS}) can discriminate between surgical outcome groups with $AUC=0.75$.

In contrast, when only using the maximum relative band power in all 62 patients without scoring it against the normative map, patients with persistent seizures (ILAE3+) were not distinguishable from seizure-free patients in any individual frequency band (ILAE1,2) (δ $p=0.28$, θ $p=0.25$, α $p=0.19$, β $p=0.78$, γ $p=0.70$). This result highlights that it is indeed the abnormality relative to the normative map that contains information on epileptogenic tissue, rather than band power *per se*.

Finally, for clinical translation, it is also important to assess the robustness of our finding towards the exact interictal segment used. We chose two additional segments of interictal data in the 62 patients, where possible, separated by at least 4 hours and at least 2 hours away from seizures. Repeating the analysis on these two additional segments showed that D_{RS} performed similarly well in discriminating between surgical outcome groups ($AUC=0.67$, $p=0.02$ and $AUC=0.71$, $p=0.005$, see Fig. 4C,D). In Supplementary Figure 1 we additionally demonstrate the robustness of our results towards different parcellation schemes. Therefore, our main findings were robust to the choice of parcellation and interictal data segment.

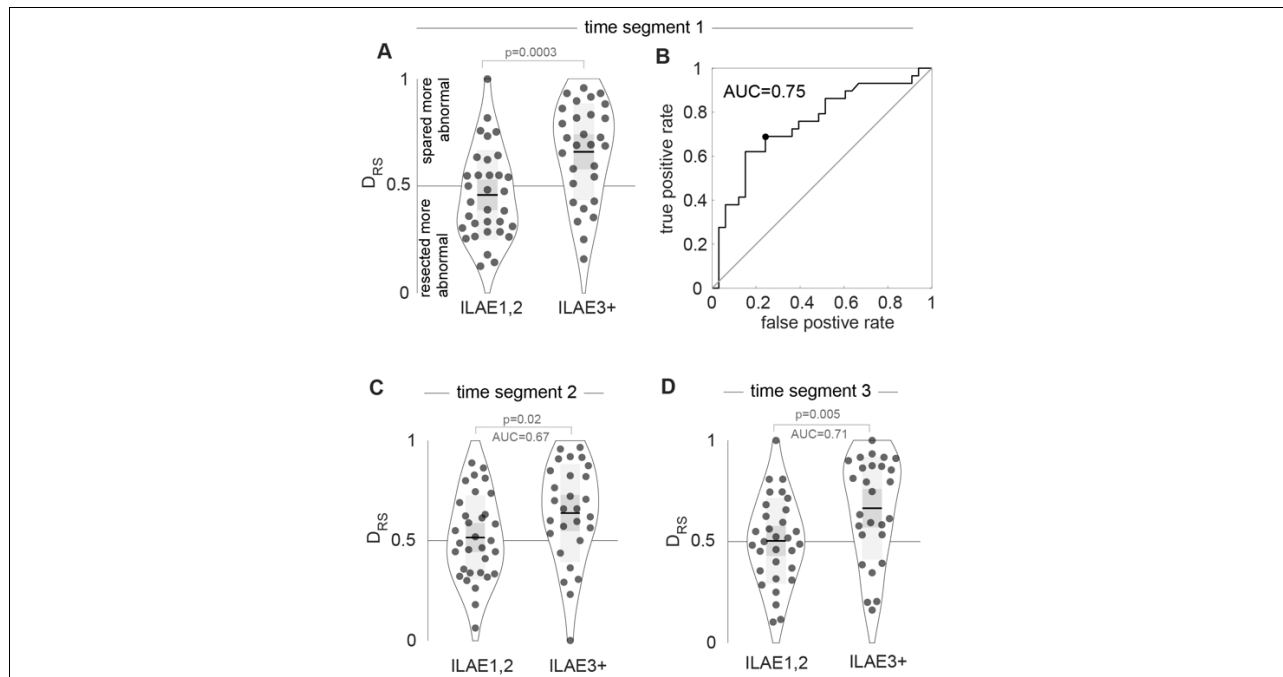


Figure 4: Interictal band power abnormality distribution in resected vs. spared tissue explains post-surgical seizure-freedom. **A.** The D_{RS} values, which indicate if resected regions were more abnormal than spared regions, for each patient separated by outcome group. At a group level the resected regions were more abnormal than spared regions in ILAE3+ patients, with substantially and significantly higher D_{RS} values. Each point is an individual patient, black horizontal line indicates the mean, grey box indicates the standard deviation. **B.** Using D_{RS} as a binary classifier

with a receiver operator characteristic curve (ROC) allows a calculation of the area under the curve (AUC) = 0.75 to predict ILAE outcome class. C., D. Replication of the findings in panel A using other data segments at least 4 hours away from the first data segment.

Discussion

In this study we derived a normative map of relative band power across the brain using intracranial EEG. The use of normative baselines is commonplace in a wide range of neurology research; however, this approach is rare for invasive modalities such as intracranial EEG. By applying an intracranial EEG normative map in the context of epilepsy presurgical evaluation, we made several key contributions. First, we derived a normative map of interictal band power for different brain regions and frequency bands using the largest dataset to date. Second, we found that we can leverage this normative map to identify regional abnormalities within individual patients. Third, by overlaying abnormal regions with knowledge of resected tissue, we validated our identified abnormalities against surgical outcomes. Finally, we also demonstrated the robustness of our results to the choice of brain parcellation and iEEG segment.

Our normative map, inferred using intracranial EEG, has striking similarities to spectral profiles observed using other modalities such as MEG and scalp EEG (Keitel and Gross 2016; Hillebrand et al. 2012; Morillon et al. 2019). Some regional frequency-specific neocortical activity patterns are well known, including alpha in parietal regions and beta in motor areas (Babiloni et al. 2010; Kilavik et al. 2013). In complement to prior scalp EEG and MEG studies, our analysis also allows the investigation of deep brain subcortical structures with high spatial accuracy. Specifically, we report strong delta power in limbic structures including the hippocampus in agreement with one previous intracranial study (Frauscher et al. 2018). Interestingly, we also found strong delta power in anterior temporal and inferior frontal areas, as reported previously (Niso et al. 2016). Given the strong connectivity within limbic, anterior temporal, and inferior frontal areas, including via the uncinate fasciculus, we suggest a potential structural underpinning for the spatial profiles observed in our normative maps. A future comparison of our normative map to a normative white-matter structural connectome could confirm this hypothesis for a given parcellation.

Few studies have used interictal intracranial recordings from multiple subjects to infer a normative brain activity. An early study by (Groppe et al. 2013) investigated data from 15 individuals and mapped spatial profiles of band power estimates. In agreement with our findings, they reported high beta power in motor areas and high theta in superior frontal areas (figure 1), amongst other spatial patterns. Perhaps most similar to our work is the study by (Frauscher et al. 2018), who created a normative map with intracranial data from 106 subjects. The authors suggested that clinical EEGs could be compared to such a map to identify abnormal activity. Our study builds on this literature by creating an atlas from 234 subjects and applying it to an independent sample of 62 patients with epilepsy.

After scoring the epilepsy cohort against the normative map, our goal was to detect abnormalities in interictal EEG activity that may help localise the epileptogenic tissue. To achieve

this, we wanted to acknowledge the diversity of possible interictal abnormalities. Therefore, we extracted the maximum absolute abnormality in any frequency band. Our proposed $\max(|z|)$ measure is only one of several measures likely to be important for epileptogenic zone localisation, and other dimensionality reduction techniques may be beneficial (Owen et al. 2020). Future studies should also investigate the band-specific abnormalities, and relate them to the subject-specific interictal activity patterns (e.g. spikes, slowing, etc.) to aid interpretation. Here, we did not specifically investigate the relationship to particular interictal activity patterns, as we wanted to demonstrate a generalisable framework that can detect interictal abnormalities regardless of the specific nature, pattern, location, or cause of the abnormality. However, it is conceivable that e.g. specific etiologies are associated with specific patterns of interictal abnormality. We also did not control for other factors such as handedness, or eyes open/closed, vigilance state, etc. due to unavailability of this information in our retrospective study design. Future work should investigate the influence of epileptiform activity, as well as various other factors known to impact band power in EEG.

Our study further contributes to a growing literature searching for pre-operative imaging markers of the epileptogenic zone that predict post-surgery patient outcomes (e.g. (Kini et al. 2019; Goodale et al. 2020; Narasimhan et al. 2020; Lagarde et al. 2018; Dauwels, Eskandar, and Cash 2009; Shah et al. 2019; Antony et al. 2013; Sinha et al. 2017a)). In general, two main approaches can be used to identify pre-operative markers. The first is to use an entirely data-driven approach. Typically, this strategy involves high dimensional data and feature selection methods (Taylor et al. 2018; Munsell et al. 2015). However, interpreting the selected features may be challenging. In the present study we instead used a hypothesis-driven approach to identify abnormal regions, which we hypothesised would remain after surgery in patients with persistent seizures. Other studies using hypothesis-driven approaches suggested removing hub regions may explain outcomes (Ramaraju et al. 2020; Wang et al. 2020), whilst using clinical demographics along with imaging has also been suggested (Bell et al. 2017; Jehi et al. 2015). We expect that combining different approaches and features will yield a translatable and interpretable biomarker of epileptogenic tissue and provide optimal predictions for post-surgical seizure-freedom (Sinha et al. 2017b).

Our normative map approach for localising epileptogenic tissue could complement current clinical analysis of intracranial EEG. Currently, one of the key parts of presurgical evaluation is localising seizure onset. However, resecting the seizure onset zone may not lead to seizure freedom in cases where the seizure onset zone and epileptogenic zone only partially overlap (Rosenow and Lüders 2001). Furthermore, seizure onset data may not be readily available, the onset location may not be consistent (King-Stephens et al. 2015), or the onset pattern may be diffuse for some patients, making it challenging or impossible to conclusively localise the epileptogenic zone using only their seizure data. Thus, to complement this approach, clinicians also evaluate interictal intracranial EEG for abnormalities such as spikes (Rosenow and Lüders 2001) and high frequency oscillations (Chen et al. 2021), which may be biomarkers of the epileptogenic zone. As discussed previously, visual inspection of intracranial EEG may miss more subtle frequency changes in neural activity, especially activity that is normal in one region may be abnormal if observed in another. By comparing interictal intracranial EEG band power to a normative map, our approach highlights less salient, region-specific aberrations, providing a complementary tool to

the traditional visual inspection of ictal and interictal EEG. Moreover, by extracting more information from interictal EEG, our approach may allow clinicians to successfully localise the epileptogenic zone in the absence of clear seizure data.

To demonstrate the clinical usefulness of our approach, we showed that the discrimination of surgical outcome groups was robust to the choice of the interictal EEG segment. However, this finding should not be mistaken as evidence that interictal band power abnormality remains stable over time; rather, it simply demonstrates that the predictive power of this measure is not sensitive to abnormality fluctuations in our cohort. Indeed, it is likely that abnormality changes over time given the known variability in interictal dynamics within patients with focal epilepsy. For example, both the rate and spatial patterns of pathological interictal events such as spikes (Karoly et al. 2016; Baud et al. 2018; Conrad et al. 2020a) and HFOs (Gliske et al. 2018a) fluctuate during intracranial recordings. Further, interictal band power changes over a range of timescales (see Panagiotopoulou et al. 2020 and references therein), and, as a result, band power abnormality will likely also fluctuate over time. Future work will investigate the magnitude and timescales of these fluctuations and determine if they hold additional information about epileptogenic tissue. In particular, abnormalities may be more salient following presurgical perturbations such as antiepileptic medication reduction or sleep deprivation (Meisel et al. 2015), as well as during patient-specific phases of circadian or multiday cycles (Karoly et al. 2016; Baud et al. 2018). Additionally, like other interictal features (Gliske et al. 2018a; Khambhati et al. 2016), temporal changes of abnormalities could also be related to variable seizure features such as seizure onset (Saggio et al. 2020) or evolution (Schroeder et al. 2020) within the same patient. Investigating such relationships could reveal additional applications for band power abnormalities, such as predicting seizure features.

Our study has several strengths and limitations. One strength is the sample sizes for both the normative map and epilepsy surgery datasets, which are some of the largest reported in the literature on intracranial EEG. Furthermore, the availability of patient data from other modalities including pre-operative MRI, CT, and post-operative MRI allowed for accurate electrode localisation and delineation of resections. The reproducibility of the normative map across parcellations, and its agreement with existing literature, is also a major strength, providing confidence in our findings. The study's limitations include the retrospective design of the study and the single-site origin of the patient data. Additionally, data regarding the brain state of the patients at the time of recording was not included in the analysis. Future studies could investigate if normative maps and outcome predictions are affected by underlying state changes such as rest, task, or sleep.

Patients undergoing invasive monitoring for surgical evaluation are typically those with the most uncertainty around where to operate, and they subsequently experience poorer outcomes as a difficult-to-treat cohort. Therefore, new ways to use invasive intracranial data are sought-after to inform and improve clinical decision making. We envisage, in future, a software tool containing a normative map to which patient data and planned resections are compared (Taylor et al. 2018). Such a tool would integrate other abnormality metrics from additional modalities including scalp EEG, MEG, or MRI (Sinha et al. 2021) and make predictions of patient outcomes using advanced computational models of brain dynamics (Proix et al. 2017; Sinha et al. 2017a). Our findings pave

the way to the use of normative intracranial baselines for clinical abnormality identification in epilepsy and beyond.

Acknowledgements

We thank members of the Computational Neurology, Neuroscience & Psychiatry Lab (www.cnp-lab.com) for discussions on the analysis and manuscript; and Catherine Scott and Roman Rodionov for helping with data organization. B.D. receives support from the NIH National Institute of Neurological Disorders and Stroke U01-NS090407 (Center for SUDEP Research) and Epilepsy Research UK. Y.W. gratefully acknowledges funding from Wellcome Trust (208940/Z/17/Z). P.N.T. is supported by a UKRI Future Leaders Fellowship (MR/T04294X/1). T.O. is supported by the Centre for Doctoral Training in Cloud Computing for Big Data (EP/L015358/1).

Figure captions

Figure 1: Normative band power varies across regions. Mean relative band power in each region for each of the five frequency bands of interest. The colour axes scale differs for each frequency band with generally higher power in lower frequencies.

Figure 2: Normative band power as a reference to detect abnormalities in individual patients. **A.** Visualisation of the regions covered by the implanted electrodes in an example patient with epilepsy. 18 of the 128 regions were sampled by the electrode contacts in this patient (black circles). Time series from two example regions are shown that are without obvious epileptiform activity (inset). One example region (left lateral occipital gyrus 2) was the seizure onset zone in this patient. **B.** Relative band power for each of the two regions, across each frequency band is plotted for the normative data (coloured violin plot; each point is a normative subject). Data is standardised (mean subtracted and divided by standard deviation). Relative band power z-score for the patient 1216 is plotted as a vertical dashed line on the same scale. The z-scores indicates that the left middle temporal gyrus is normal in all frequency bands (maximum absolute z-score = 1.04). The left lateral occipital gyrus is more abnormal in theta (maximum absolute z-score = 2.99) and gamma (absolute z-score = 1.59). **C.** Maximum absolute z-score for each region plotted for the patient. Larger values indicate greater abnormality in any frequency band.

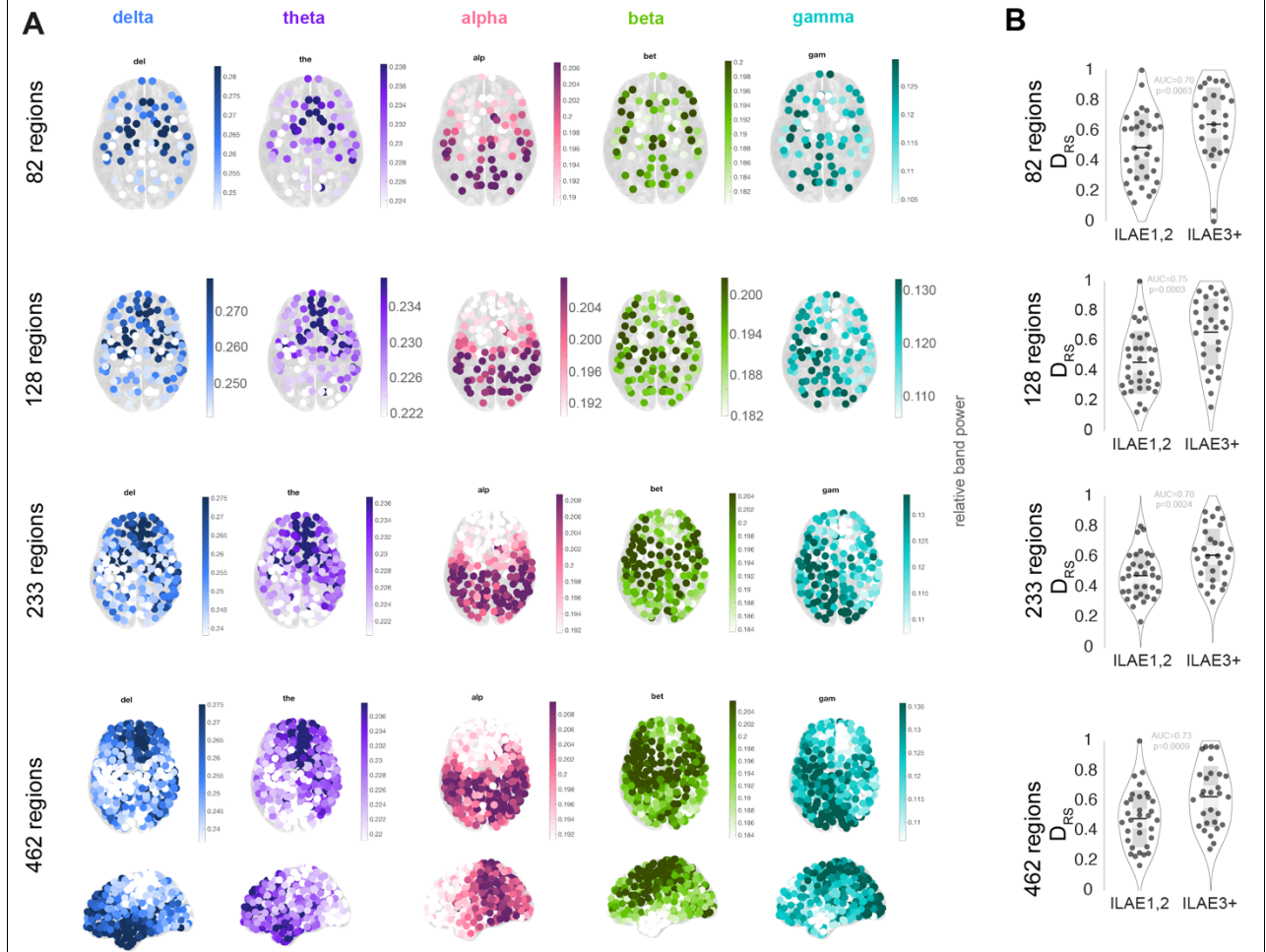
Figure 3: Interictal band power abnormality as a marker of epileptogenic tissue in two example patients. **A, C** Post-operative T1-weighted MRI scans showing the location of the resection as indicated by the green arrow. **B.** Replication of the patient in figure 2 with the regions that were later surgically resected circled in black. Non-resected regions are circled in white. A direct comparison and quantification in the lower panel shows resected regions to be more abnormal than spared. Each data point is a separate region. This patient was seizure free after surgery (ILAE1). **D.** Visualisation of data from a second patient with a frontal lobe implantation. Multiple abnormal regions were present outside the resection and spared by surgery. This patient had had continued post-operative seizures (ILAE4). In both patients the D_{RS} metric quantified the difference between resected and spared regions in terms of their abnormality.

Figure 4: Interictal band power abnormality distribution in resected vs. spared tissue explains post-surgical seizure-freedom. **A.** The D_{RS} values, which indicate if resected regions were more abnormal than spared regions, for each patient separated by outcome group. At a group level the resected regions were more abnormal than spared regions in ILAE3+ patients, with substantially and significantly higher D_{RS} values. Each point is an individual patient, black horizontal line indicates the mean, grey box indicates the standard deviation. **B.** Using D_{RS} as a binary classifier with a receiver operator characteristic curve (ROC) allows a calculation of the area under the curve (AUC) = 0.75 to predict ILAE outcome class. **C., D.** Replication of the findings in panel A using other data segments at least 4 hours away from the first data segment.

Supplementary Information

Table S1 Detailed patient data.

Figure S1: Replication of findings across parcellations A. Normative maps replicated for four different parcellations. The second row uses identical data to that shown in figure 1. B. Replication of surgical outcome findings across parcellations.



References

- Antony, Arun R, Andreas V Alexopoulos, Jorge A González-Martínez, John C Mosher, Lara Jehi, Richard C Burgess, Norman K So, and Roberto F Galán. 2013. "Functional Connectivity Estimated from Intracranial EEG Predicts Surgical Outcome in Intractable Temporal Lobe Epilepsy." *PloS One* 8 (10): e77916.
- Babiloni, Claudio, Nicola Marzano, Marco Iacoboni, Francesco Infarinato, Pierluigi Aschieri, Paola Buffo, Giuseppe Cibelli, Andrea Soricelli, Fabrizio Eusebi, and Claudio Del Percio. 2010. "Resting State Cortical Rhythms in Athletes: A High-Resolution EEG Study." *Brain Research Bulletin* 81 (1): 149–56.
- Baud, Maxime O., Jonathan K. Kleen, Emily A. Mirro, Jason C. Andrechak, David King-Stephens, Edward F. Chang, and Vikram R. Rao. 2018. "Multi-Day Rhythms Modulate Seizure Risk in Epilepsy." *Nature Communications* 9 (1): 1–10.
- Bell, Gail S, Jane de Tisi, Juan Carlos Gonzalez-Fraile, Janet L Peacock, Andrew W McEvoy, William FJ Harkness, Jacqueline Foong, et al. 2017. "Factors Affecting Seizure Outcome After Epilepsy Surgery: An Observational Series." *Journal of Neurology, Neurosurgery & Psychiatry* 88 (11): 933–40.
- Bernabei, John M, Thomas Campbell Arnold, Preya Shah, Andrew Revell, Ian Z Ong, Lohith Kini, Joel M Stein, et al. 2020. "Electrocorticography and Stereo EEG Provide Distinct Measures of Brain Connectivity: Implications for Network Models." *medRxiv*.
- Betzal, Richard F, John D Medaglia, Ari E Kahn, Jonathan Soffer, Daniel R Schonhaut, and Danielle S Bassett. 2019. "Structural, Geometric and Genetic Factors Predict Interregional Brain Connectivity Patterns Probed by Electrocorticography." *Nature Biomedical Engineering* 3 (11): 902–16.
- Chen, Zhuying, Matias I Maturana, Anthony N Burkitt, Mark J Cook, and David B Grayden. 2021. "High-Frequency Oscillations in Epilepsy: What Have We Learned and What Needs to Be Addressed." *Neurology* 96 (9): 439–48.
- Conrad, Erin C., Samuel B. Tomlinson, Jeremy N. Wong, Kelly F. Oechel, Russell T. Shinohara, Brian Litt, Kathryn A. Davis, and Eric D. Marsh. 2020a. "Spatial Distribution of Interictal Spikes Fluctuates over Time and Localizes Seizure Onset." *Brain* 143 (2): 554–69. <https://doi.org/10.1093/brain/awz386>.
- Conrad, Erin C, Samuel B Tomlinson, Jeremy N Wong, Kelly F Oechel, Russell T Shinohara, Brian Litt, Kathryn A Davis, and Eric D Marsh. 2020b. "Spatial Distribution of Interictal Spikes Fluctuates over Time and Localizes Seizure Onset." *Brain* 143 (2): 554–69.
- Dauwels, Justin, Emad Eskandar, and Sydney Cash. 2009. "Localization of Seizure Onset Area from Intracranial Non-Seizure EEG by Exploiting Locally Enhanced Synchrony." In *2009 Annual International Conference of the IEEE Engineering in Medicine and Biology Society*, 2180–83. IEEE.

Durnford, Andrew J, William Rodgers, Fenella J Kirkham, Mark A Mullee, Andrea Whitney, Martin Prevett, Lucy Kinton, Matthew Harris, and William P Gray. 2011. "Very Good Inter-Rater Reliability of Engel and ILAE Epilepsy Surgery Outcome Classifications in a Series of 76 Patients." *Seizure* 20 (10): 809–12.

Frauscher, Birgit, Nicolas Von Ellenrieder, Rina Zelmann, Irena Doležalová, Lorella Minotti, André Olivier, Jeffery Hall, et al. 2018. "Atlas of the Normal Intracranial Electroencephalogram: Neurophysiological Awake Activity in Different Cortical Areas." *Brain* 141 (4): 1130–44.

Gliske, Stephen V., Zachary T. Irwin, Cynthia Chestek, Garnett L. Hegeman, Benjamin Brinkmann, Oren Sagher, Hugh J. L. Garton, Greg A. Worrell, and William C. Stacey. 2018a. "Variability in the Location of High Frequency Oscillations During Prolonged Intracranial EEG Recordings." *Nature Communications* 9 (1): 2155.

Gliske, Stephen V, Zachary T Irwin, Cynthia Chestek, Garnett L Hegeman, Benjamin Brinkmann, Oren Sagher, Hugh JL Garton, Greg A Worrell, and William C Stacey. 2018b. "Variability in the Location of High Frequency Oscillations During Prolonged Intracranial EEG Recordings." *Nature Communications* 9 (1): 1–14.

Goodale, Sarah E, Hernán FJ González, Graham W Johnson, Kanupriya Gupta, William J Rodriguez, Robert Shults, Baxter P Rogers, et al. 2020. "Resting-State SEEG May Help Localize Epileptogenic Brain Regions." *Neurosurgery* 86 (6): 792–801.

Groppe, David M, Stephan Bickel, Corey J Keller, Sanjay K Jain, Sean T Hwang, Cynthia Harden, and Ashesh D Mehta. 2013. "Dominant Frequencies of Resting Human Brain Activity as Measured by the Electrocorticogram." *Neuroimage* 79: 223–33.

Hagmann, Patric, Leila Cammoun, Xavier Gigandet, Reto Meuli, Christopher J Honey, Van J Wedeen, and Olaf Sporns. 2008. "Mapping the Structural Core of Human Cerebral Cortex." *PLoS Biol* 6 (7): e159.

Hamilton, Liberty S, David L Chang, Morgan B Lee, and Edward F Chang. 2017. "Semi-Automated Anatomical Labeling and Inter-Subject Warping of High-Density Intracranial Recording Electrodes in Electrocorticography." *Frontiers in Neuroinformatics* 11: 62.

Hatton, Sean N, Khoa H Huynh, Leonardo Bonilha, Eugenio Abela, Saud Alhusaini, Andre Altmann, Marina KM Alvim, et al. 2020. "White Matter Abnormalities Across Different Epilepsy Syndromes in Adults: An ENIGMA Epilepsy Study." *Brain* 143 (8): 2454–73.

Hillebrand, Arjan, Gareth R Barnes, Johannes L Bosboom, Henk W Berendse, and Cornelis J Stam. 2012. "Frequency-Dependent Functional Connectivity Within Resting-State Networks: An Atlas-Based MEG Beamformer Solution." *Neuroimage* 59 (4): 3909–21.

Hufnagel, Andreas, Christian E Elger, Hendrik Pels, Joseph Zentner, Helmut K Wolf, Johannes Schramm, and Otmar D Wiestler. 1994. "Prognostic Significance of Ictal and Interictal Epileptiform Activity in Temporal Lobe Epilepsy." *Epilepsia* 35 (6): 1146–53.

Ishii, Ryouhei, Kazuhiro Shinosaki, Satoshi Ukai, Tsuyoshi Inouye, Tsutomu Ishihara, Toshiki Yoshimine, Norio Hirabuki, et al. 1999. "Medial Prefrontal Cortex Generates Frontal Midline Theta Rhythm." *Neuroreport* 10 (4): 675–79.

Jacobs, Julia, Pierre LeVan, Claude-Édouard Châtillon, André Olivier, François Dubeau, and Jean Gotman. 2009. "High Frequency Oscillations in Intracranial EEGs Mark Epileptogenicity Rather Than Lesion Type." *Brain* 132 (4): 1022–37.

Jacobs, Julia, Maeike Zijlmans, Rina Zelmann, Claude-Édouard Chatillon, Jeffrey Hall, André Olivier, François Dubeau, and Jean Gotman. 2010. "High-Frequency Electroencephalographic Oscillations Correlate with Outcome of Epilepsy Surgery." *Annals of Neurology: Official Journal of the American Neurological Association and the Child Neurology Society* 67 (2): 209–20.

Jehi, Lara, Ruta Yardi, Kevin Chagin, Laura Tassi, Giorgio Lo Russo, Gregory Worrell, Wei Hu, et al. 2015. "Development and Validation of Nomograms to Provide Individualised Predictions of Seizure Outcomes After Epilepsy Surgery: A Retrospective Analysis." *The Lancet Neurology* 14 (3): 283–90.

Karoly, Philippa J., Dean R. Freestone, Ray Boston, David B. Grayden, David Himes, Kent Leyde, Udaya Seneviratne, Samuel Berkovic, Terence O'Brien, and Mark J. Cook. 2016. "Interictal Spikes and Epileptic Seizures: Their Relationship and Underlying Rhythmicity." *Brain* 139 (4): 1066–78.

Keitel, Anne, and Joachim Gross. 2016. "Individual Human Brain Areas Can Be Identified from Their Characteristic Spectral Activation Fingerprints." *PLoS Biology* 14 (6): e1002498.

Khambhati, Ankit N, Kathryn A Davis, Timothy H Lucas, Brian Litt, and Danielle S Bassett. 2016. "Virtual Cortical Resection Reveals Push-Pull Network Control Preceding Seizure Evolution." *Neuron* 91 (5): 1170–82.

Kilavik, Bjørg Elisabeth, Manuel Zaepffel, Andrea Brovelli, William A MacKay, and Alexa Riehle. 2013. "The Ups and Downs of Beta Oscillations in Sensorimotor Cortex." *Experimental Neurology* 245: 15–26.

King-Stephens, David, Emily Mirro, Peter B. Weber, Kenneth D. Laxer, Paul C. Van Ness, Vicenta Salanova, David C. Spencer, et al. 2015. "Lateralization of Mesial Temporal Lobe Epilepsy with Chronic Ambulatory Electrocorticography." *Epilepsia* 56 (6): 959–67.

Kini, Lohith G, John M Bernabei, Fadi Mikhail, Peter Hadar, Preya Shah, Ankit N Khambhati, Kelly Oechsel, et al. 2019. "Virtual Resection Predicts Surgical Outcome for Drug-Resistant Epilepsy." *Brain* 142 (12): 3892–3905.

Klooster, Maryse A van't, Nicole EC van Klink, Willemiek JEM Zweiphenning, Frans SS Leijten, Rina Zelmann, Cyrille H Ferrier, Peter C van Rijen, et al. 2017. "Tailoring Epilepsy Surgery with Fast Ripples in the Intraoperative Electrocorticogram." *Annals of Neurology* 81 (5): 664–76.

Lagarde, Stanislas, Nicolas Roehri, Isabelle Lambert, Agnès Trebuchon, Aileen McGonigal, Romain Carron, Didier Scavarda, et al. 2018. "Interictal Stereotactic-EEG Functional Connectivity in Refractory Focal Epilepsies." *Brain* 141 (10): 2966–80.

Lancaster, Jack L, Diana Tordesillas-Gutiérrez, Michael Martinez, Felipe Salinas, Alan Evans, Karl Zilles, John C Mazziotta, and Peter T Fox. 2007. "Bias Between MNI and Talairach Coordinates Analyzed Using the ICBM-152 Brain Template." *Human Brain Mapping* 28 (11): 1194–1205.

Meisel, Christian, Andreas Schulze-Bonhage, Dean Freestone, Mark James Cook, Peter Achermann, and Dietmar Plenz. 2015. "Intrinsic Excitability Measures Track Antiepileptic Drug Action and Uncover Increasing/Decreasing Excitability over the Wake/Sleep Cycle." *Proceedings of the National Academy of Sciences* 112 (47): 14694–99.

Morillon, Benjamin, Luc H Arnal, Charles E Schroeder, and Anne Keitel. 2019. "Prominence of Delta Oscillatory Rhythms in the Motor Cortex and Their Relevance for Auditory and Speech Perception." *Neuroscience & Biobehavioral Reviews* 107: 136–42.

Munsell, Brent C, Chong-Yaw Wee, Simon S Keller, Bernd Weber, Christian Elger, Laura Angelica Tomaz da Silva, Travis Nesland, Martin Styner, Dinggang Shen, and Leonardo Bonilha. 2015. "Evaluation of Machine Learning Algorithms for Treatment Outcome Prediction in Patients with Epilepsy Based on Structural Connectome Data." *Neuroimage* 118: 219–30.

Narasimhan, Saramati, Keshav B Kundassery, Kanupriya Gupta, Graham W Johnson, Kristin E Wills, Sarah E Goodale, Kevin Haas, et al. 2020. "Seizure-Onset Regions Demonstrate High Inward Directed Connectivity During Resting-State: An SEEG Study in Focal Epilepsy." *Epilepsia* 61 (11): 2534–44.

Niso, Guiomar, Christine Rogers, Jeremy T Moreau, Li-Yuan Chen, Cecile Madjar, Samir Das, Elizabeth Bock, et al. 2016. "OMEGA: The Open MEG Archive." *Neuroimage* 124: 1182–87.

Niso, Guiomar, Francois Tadel, Elizabeth Bock, Martin Cousineau, Andrés Santos, and Sylvain Baillet. 2019. "Brainstorm Pipeline Analysis of Resting-State Data from the Open MEG Archive." *Frontiers in Neuroscience* 13: 284.

Owen, Thomas W, Jane de Tisi, Sjoerd B Vos, Gavin P Winston, John S Duncan, Yujiang Wang, and Peter N Taylor. 2020. "Multivariate White Matter Alterations Are Associated with Epilepsy Duration." *European Journal of Neuroscience*.

Panagiotopoulou, Mariella, Christoforos Pappasavvas, Gabrielle M. Schroeder, Peter Taylor, and Yujiang Wang. 2020. "Fluctuations in EEG Band Power over Minutes to Days Explain How Seizures Change over Time." *arXiv:2012.07105 [q-Bio]*, December.

Proix, Timothée, Fabrice Bartolomei, Maxime Guye, and Viktor K Jirsa. 2017. "Individual Brain Structure and Modelling Predict Seizure Propagation." *Brain* 140 (3): 641–54.

Ramaraju, Sriharsha, Yujiang Wang, Nishant Sinha, Andrew W McEvoy, Anna Miserocchi, Jane De Tisi, John S Duncan, Fergus Rugg-Gunn, and Peter N Taylor. 2020. "Removal of Interictal MEG-

Derived Network Hubs Is Associated with Postoperative Seizure Freedom.” *Frontiers in Neurology* 11.

Roehri, Nicolas, Francesca Pizzo, Stanislas Lagarde, Isabelle Lambert, Anca Nica, Aileen McGonigal, Bernard Giusiano, Fabrice Bartolomei, and Christian-George Bénar. 2018. “High-Frequency Oscillations Are Not Better Biomarkers of Epileptogenic Tissues Than Spikes.” *Annals of Neurology* 83 (1): 84–97.

Rosenow, Felix, and Hans Lüders. 2001. “Presurgical Evaluation of Epilepsy.” *Brain* 124 (9): 1683–1700.

Saggio, Maria Luisa, Dakota Crisp, Jared Scott, Phillippa J. Karoly, Levin Kuhlmann, Mitsuyoshi Nakatani, Tomohiko Murai, et al. 2020. “Epidynamics Characterize and Navigate the Map of Seizure Dynamics.” *bioRxiv*, February, 2020.02.08.940072.

Schroeder, Gabrielle M, Beate Diehl, Fahmida A Chowdhury, John S Duncan, Jane De Tisi, Andrew J Trevelyan, Rob Forsyth, Andrew Jackson, Peter N Taylor, and Yujiang Wang. 2020. “Seizure Pathways Change on Circadian and Slower Timescales in Individual Patients with Focal Epilepsy.” *Proceedings of the National Academy of Sciences* 117 (20): 11048–58.

Shah, Preya, John M Bernabei, Lohith G Kini, Arian Ashourvan, Jacqueline Boccanfuso, Ryan Archer, Kelly Oechsel, et al. 2019. “High Interictal Connectivity Within the Resection Zone Is Associated with Favorable Post-Surgical Outcomes in Focal Epilepsy Patients.” *NeuroImage: Clinical* 23: 101908.

Sinha, Nishant, Justin Dauwels, Marcus Kaiser, Sydney S Cash, M Brandon Westover, Yujiang Wang, and Peter N Taylor. 2017a. “Predicting Neurosurgical Outcomes in Focal Epilepsy Patients Using Computational Modelling.” *Brain* 140 (2): 319–32.

Sinha, Nishant, Justin Dauwels, Marcus Kaiser, Sydney S Cash, M Brandon Westover, Yujiang Wang, and Peter N Taylor. 2017b. “Reply: Computer Models to Inform Epilepsy Surgery Strategies: Prediction of Postoperative Outcome.” *Brain* 140 (5): e31–31.

Sinha, Nishant, Yujiang Wang, Nádia Moreira da Silva, Anna Miserocchi, Andrew W McEvoy, Jane de Tisi, Sjoerd B Vos, Gavin P Winston, John S Duncan, and Peter N Taylor. 2021. “Structural Brain Network Abnormalities and the Probability of Seizure Recurrence After Epilepsy Surgery.” *Neurology* 96 (5): e758–71.

Taylor, Peter N, Nishant Sinha, Yujiang Wang, Sjoerd B Vos, Jane de Tisi, Anna Miserocchi, Andrew W McEvoy, Gavin P Winston, and John S Duncan. 2018. “The Impact of Epilepsy Surgery on the Structural Connectome and Its Relation to Outcome.” *NeuroImage: Clinical* 18: 202–14.

Wang, Yujiang, Nishant Sinha, Gabrielle M Schroeder, Sriharsha Ramaraju, Andrew W McEvoy, Anna Miserocchi, Jane de Tisi, et al. 2020. “Interictal Intracranial Electroencephalography for Predicting Surgical Success: The Importance of Space and Time.” *Epilepsia* 61 (7): 1417–26.

Whelan, Christopher D, Andre Altmann, Juan A Botía, Neda Jahanshad, Derrek P Hibar, Julie Absil, Saud Alhusaini, et al. 2018. "Structural Brain Abnormalities in the Common Epilepsies Assessed in a Worldwide ENIGMA Study." *Brain* 141 (2): 391–408.